Title **Improved continuous fumaric acid production with immobilised *Rhizopus oryzae* by implementation of a revised nitrogen control strategy**

Authors Andre Naude

Willie Nicol

Affiliation Department of Chemical Engineering, University of Pretoria, Lynwood Road, Hatfield, 0002 Pretoria, South Africa

Corresponding author: Willie Nicol

Tel: +27124203796; Fax: +27124205048

Email: willie.nicol@up.ac.za, willie.nicol@gmail.com

Highlights

- A new nitrogen control mechanism is proposed where nitrogen is fed continuously.
- Ethanol production decreased over time at low urea feed rates (0.625mgL−1h−1).
- Fumaric acid production only showed a slight decrease at low urea feed rates.
- An instantaneous yield of 0.96gg−1 was achieved at low urea feed rates.

Abstract

A novel fermentation system was employed whereby the mycelial mat of *Rhizopus oryzae* was attached to a polypropylene tube. Batch operation was used for growth, while continuous operation was employed during the fumaric acid production phase. A clear decrease in respiration, fumaric acid (FA) and ethanol production was observed when zero nitrogen was fed in the production phase, with FA productivity decreasing from an initial 0.7 $g.L^{-1}.h^{-1}$ to 0.3 $g.L^{-1}.h^{-1}$ after 150 hours. With the addition of 0.625 $mg.L^{-1}.h^{-1}$ of urea FA productivity dropped to only 0.4 $g.L^{-1}.h^{-1}$ after 150 hours and 0.3 $g.L^{-1}.h^{-1}$ after 400 hours. Under these conditions it was observed that the ethanol production rate decreased 20 times faster compared with the FA production rate, therefore resulting in high FA yields towards the end of the fermentation (instantaneous 0.96 $g.g^{-1}$ and average 0.81 $g.g^{-1}$ after 400 hours). Increasing the urea feed rate to 1.875 $mg.L^{-1}.h^{-1}$ resulted in a clear increase in FA production and respiration rates. This condition also resulted in a 25% increase in biomass after 150 hours, while the decline in the ethanol production rate was seven times lower than in the 0.625 $mg.L^{-1}.h^{-1}$ urea fermentation, resulting in lower FA yields.

Keywords

Fumaric acid; Fermentation; Immobilisation; Bioreactors; *Rhizopus oryzae*

Nomenclature

A	decay factor
ATP	adenosine triphosphate
C_L	liquid phase (HPLC) concentration ($g.L^{-1}$)
C_G	gas analyser concentration (%)
C_{G0}	inlet gas concentration (%)
D_G	gas phase dilution rate (h^{-1})
D_{L0}	inlet liquid dilution rate (h^{-1})
D_L	liquid dilution rate (h^{-1})
eth	ethanol
FA	fumaric acid
Gly	glycerol
NADH	nicotinamide adenine dinucleotide
P	atmospheric pressure (kPa)
R	ideal gas constant
r	volumetric productivity ($g.L^{-1}.h^{-1}$ [liquid], $mmol.h^{-1}.L^{-1}$[gas])
r_g	mass based glucose consumption rate ($g.g\ biomass^{-1}.h^{-1}$)
r_{INIT}	initial volumetric productivity ($g.L^{-1}.h^{-1}$ [liquid], $mmol.h^{-1}.L^{-1}$ [gas])
SA	succinic acid
T	temperature

Y	Yield factor

Introduction

Fumaric acid (FA) is a four-carbon unsaturated dicarboxylic acid and is present in the tricarboxylic acid cycle. FA has been identified by the USA Department of Energy as one of the top 12 chemicals to be produced by industrial fermentation from renewable substrates [1]. Fumaric acid is used extensively; examples include synthetic resins and biodegradable polymers in the polymer industry [2], as a food acidulent and beverage ingredient in the food industry [3] and as an antibacterial agent in the pharmaceutical industry [3]. The most significant future application would be in the production of maleic anhydride from FA. Maleic anhydride currently has a market size of 2.1 Mton per annum [4]. FA is currently produced from butane in the petrochemical industry but due to environmental considerations, fermentation-based routes are receiving more interest [2].

The filamentous fungus *Rhizopus oryzae* (ATCC 20344) has been shown to be the top microbial FA producer and has been used the most widely in the open literature [2,3,5] utilising various substrates including glucose, xylose and plant hydrolysates [3,6,7]. Attempts at FA production with better known genetically modified microbes are still not able to compete with production with *Rhizopus oryzae* (ATCC 20344) [8,9]. The majority of fermentations with *R.oryzae* use two stages.In the first stage (growth stage), the fungus is grown aerobically in order to produce small mycelial pellets. The second stage (production stage) is an aerobic, non-growth stage in which FA production is induced by phosphate or nitrogen limitation [10–13]. Unlike most other microbes, the glucose consumption rate does not drop significantly with the onset of phosphate/nitrogen limitation. Instead the glucose is redirected towards FA production since the pathway is both adenosine triphosphate (ATP) and nicotinamide adenine dinucleotide (NADH) neutral, i.e. there is no net production/consumption of NADH or ATP when FA is produced from glucose by *R. oryzae* [14]. The metabolic pathways which are active during the FA production was illustrated in our previous work [15].

Ethanol is an unwanted by-product during the production stage. This has been associated with oxygen diffusion limitations within the biomass [2,12]. Because of this, the majority of studies on *R. oryzae* focus on reducing ethanol production by manipulating the morphology of *R. oryzae*, with the focus on

optimising the growth phase parameters (pH, dissolved oxygen, metal ion concentration and shear conditions) in order to decrease the diameter of the mycelial pellets. Although these studies have made considerable progress in reducing the size of the mycelial pellets, none have reported a significant reduction in ethanol production [10–12,16–18]. The result is that the FA yields obtained (glucose as substrate) with the pellet morphology are still low (0.3 $g.g^{-1}$–0.6 $g.g^{-1}$) compared with the theoretical maximum of 1.28 $g.g^{-1}$ [3]. Owing to these poor yields, the focus has shifted towards other means of reducing ethanol production. Studies conducted by our research group indicate that the ethanol production rate decreases significantly over time compared with the FA production rate, resulting in an increase in the FA yield over time [15]. This phenomenon is also present in the data of other authors [3,12,18,19], but has not been reported on. Manipulating the production phase to increase the fermentation time could lead to significant gains in FA yield. Switching from batch to continuous operation could lead to prolonged fermentation time in the production phase. However, there have been no published studies on continuous FA production, since the pellet morphology causes significant operational issues, such as blockage in the reactor due to mycelial pellets clumping together [3]. Switching to an immobilised system is therefore required for continuous operation.

Research on nitrogen addition in continuous citric acid production by *Aspergillus niger* shows that the operation time can be prolonged by continuous addition of nitrogen at very low feed rates [20]. Nitrogen addition during continuous FA production is therefore expected to be a very important parameter since nitrogen limitation also directly influences the flux of glucose towards FA [21,22]. Moreover, nitrogen addition is also expected to influence the length of continuous fermentation. However, even though nitrogen limitation is one of the most important mechanisms for FA production with *R. oryzae,* only two studies have been published on the topic [21,22]. Both of these used batch fermentation with high initial urea concentrations (0.1 $g.L^{-1}$ – 2 $g.L^{-1}$). However, they came to the same conclusion, namely that a urea concentration of 0.1 $g.L^{-1}$ led to optimal FA production. Since the optimum was found at the edge of the range of urea concentrations tested, it is possible that an even lower urea feed could have resulted in increased FA production.

Here, *R. oryzae* was immobilised on a polypropylene pipe. The morphology was controlled by the initial glucose concentration during the growth stage; higher glucose concentrations resulted in thicker fungal mats. During the production stage, the reactor was operated continuously. The goal was to study the influence of the continuous addition of nitrogen (urea) on the metabolism of *R. oryzae* during the production stage of continuous FA fermentation. Once an ideal nitrogen feed rate has been identified the dilution rate will be varied in order to study its effect on the metabolism. The viability of long, continuous fermentations was also investigated.

Materials and methods

Microorganism and culture conditions

R. oryzae (ATCC 20344) was prepared as described previously by Naude and Nicol [15].

Media

The growth medium consisted of (in units of $g.L^{-1}$): 4 glucose, 2 urea, 0.6 KH_2PO_4, 0.25 $MgSO_4.7H_2O$ and 0.088 $ZnSO_4.7H_2O$. The fermentation medium consisted of (in units of $g.L^{-1}$): 50 glucose, 0.6 KH_2PO_4, 0.25 $MgSO_4$ and 0.088 $ZnSO_4.7H_2O$. The urea for the nitrogen feed rate investigation was fed separately. The urea concentration used in all fermentations was 250 $mg.L^{-1}$. All media components were obtained from Merck (South Africa). Distilled water was used and all media were sterilised in an autoclave at 121 °C for 60 minutes. The glucose and urea were sterilised separately from the rest of the components.

Fermentation

The reactor, pictured in Figure 1, was a modified version of that used by Naude and Nicol [15]. The major modifications are described below. The working volume of the reactor was increased to 410 mL and the length of the polypropylene pipe was increased to 350mm.The polypropylene pripe had an outer diameter of 34 mm.

A custom, dry gas mixture (Afrox, South Africa) of 18.5% O_2, 9% CO_2 and 72.5% N_2, was sparged through the reactor. Air flow into the reactor was controlled at 40 mL.min^{-1}using a SLA5850 (Brooks, USA) mass flow controller. The gas phase of the reactor had a volume of 2.9 L. Atmospheric pressure was 86 kPa. The pH, temperature and DO were controlled at 5, 35 °C and 60% saturation respectively for both the growth and production phases as previously described [15]. The pH was controlled by dosing 10M of NaOH (to increase pH) or 1M of HCL (to decrease pH).

Growth phase

The primary goal during the growth phase was to develop a thin biofilm which would be spread evenly over the surface of the polypropylene pipe. The same growth process was used as previously described [15]. The surface area for growth was 0.068 m^2 and at the end of the growth phase the fungal mat was between 1 mm and 2 mm thick with no visible biomass present in the liquid phase i.e. all of the biomass was immobilised.

Production phase

The switch to the production phase was made once the on-line measurements indicated that all of the glucose used in the growth stage was consumed; the procedure described previously [15] was used. The reactor was operated continuously during the production phase with the nitrogen source (urea) continuously added in a separate line from the rest of the other components. This was crucial in preventing nitrogen buildup in the reactor and ensured that the biomass was exposed to a constant nitrogen concentration at all times.

Analytical methods

The procedure described earlier [15]was used to determine the glucose, fumaric acid, ethanol, malic acid, glycerol and succinic acid concentrations in the broth by means of HPLC (High Performance Liquid Chromotahraphy) with an Aminex HPX-87H ion exchange column (Bio-Rad Laboratories, USA). The CO_2 and O_2 in the outlet gas was measured using a Tandem gas analyser (Magellan

Biotech, UK) as described previously [15]. The immobilised biomass was also determined using previously described methods [15].

Results and Discussion

Model description

In continuous free-cell fermentations, volumetric productivities remain constant once the reactor has reached steady state. However, with the continuous immobilised fungal fermentation, there was a decrease in volumetric productivity over time which had to be taken into consideration. This decrease was not caused by a washout problem since the biomass was immobilised and there was no visible biomass in the fermentation outlet. As will be made clear in the discussion, it is believed that this decrease in volumetric productivity is a result of the nitrogen limitation. The growth phase was identical for all fermentations, and all biomass measurements at the end of the production phase indicated either identical biomass or a higher amount of biomass compared with those measured directly after the growth phase, i.e. growth during the production stage was limited with the majority of the carbon (> 98%) used in the production of catabolites.

Previous studies have shown that the metabolism of *R. oryzae* during FA production can be divided into three parts [3,14], namely reductive tricarboxylic acid (TCA) cycle, ethanol production and respiration (oxidative TCA together with oxidative phosphorylation). These pathways are described by Equations 1, 2 and 3. It was found that the relative volumetric rates between these three pathways were not constant throughout the fermentation, and therefore an independent rate had to be used for each one. The reductive TCA cycle, ethanol production and respiration were represented by fits on the FA, ethanol and O_2 profiles respectively. By using HPLC data, online dosing and gas profiles (O_2 and CO_2) it was found that the three main metabolic rates (FA, ethanol and O_2) were best described by the functions in Equations 4, 5 and 6. These functions are similar to those used by Ochsenreither et al. [23]. The decay factors (A_{FA}, A_{eth}, A_{O2}) in Equations 4, 5 and 6 are an indication of the fraction of the rate that is lost every hour, i.e. if a decay factor of 1% is used, it implies that 1% of the current

volumetric rate will be lost after one hour. Therefore, lower decay rates are indicative of a more stable flux towards the specified metabolite. The initial volumetric rates (r_{INIT}) in Equations 4,5 and 6 are equal to the volumetric rates at the start of the production phase ($t = 0$).

Reductive TCA $$C_6H_{12}O_6 + 2CO_2 \rightarrow 2C_4H_4O_4 + 2H_2O \quad (1)$$

Ethanol $$C_6H_{12}O_6 \rightarrow 2C_2H_6O + 2CO_2 \quad (2)$$

Respiration $$C_6H_{12}O_6 + 6O_2 \rightarrow 6CO_2 + 6H_2O \quad (3)$$

$$r_{FA} = r_{INIT_{FA}}(1 - A_{FA})^t \quad (4)$$

$$r_{eth} = r_{INIT_{eth}}(1 - A_{eth})^t \quad (5)$$

$$r_{O_2} = r_{INIT_{O_2}}(1 - A_{O_2})^t \quad (6)$$

The volumetric production rates for succinic acid (SA) and glycerol exhibited a constant ratio to that of fumaric acid. Therefore, the production rates of glycerol (Equation 7) and SA (Equation 8) are described by the fumaric acid rate with yield factors Y_{FG} and Y_{FSA} respectively. Overall, SA and glycerol were only detected in low concentrations. Pyruvic acid and malic acid are the other two minor by-products that were detected. Their data are not shown since the concentrations were too low (<0.05 $g.L^{-1}$) to generate repeatable concentration profiles.

$$r_{glyc} = Y_{FG}r_{FA} \quad (7)$$

$$r_{SA} = Y_{FSA}r_{FA} \quad (8)$$

Since steady-state analysis could not be used, due to the decreasing volumetric rates over time, dynamic analysis was used to relate the volumetric production rates (r) to the HPLC and gas analyser concentrations [24]. Equations 9 and 10 describe the liquid phase and gas phase dynamics respectively. Note that the liquid and gas phases each had their own holdups and dilution rates. The units for the liquid phase volumetric rates (r) are given in $g.L^{-1}.h^{-1}$, and those for the gas phase (CO_2

and O_2) are in mmol.L^{-1}.h^{-1}. Note that the liquid holdup was used as the basis for both of these rates. For the liquid phase, the outlet dilution rate was always higher than the inlet dilution rate due to NaOH dosing and the separate nitrogen addition. For the gas phase, it was assumed that the inlet and outlet gas volumetric flow rates were equal. The ideal gas law was used.

$$\frac{dC_L}{dt} = D_{L_0}C_{H_0} - D_L C_H + r_H \quad (9)$$

$$\frac{dC_G}{dt} = D_G(C_{G_0} - C_G) + \frac{RT}{PV_G} r_G V_L \quad (10)$$

Since the system has a double over–specification, the validity and accuracy of the model can be tested [24]. The glucose HPLC data and CO_2 gas analysis can be compared against the values predicted by the model in order to check the consistency of the overall model. The fitted rates (Equations 4, 5 and 6) are used with the stoichiometries (Equations 1, 2 and 3) to calculate the glucose consumption rate. Considering that glucose was the only substrate, the accuracy of the glucose fit (Equation 11) provides a good indication of the mass balance closures. It should be noted that r_{O2} in Equation 11 has units of mmol.L^{-1}.h^{-1} while all the other rates in Equation 11 have units of g.L^{-1}.h^{-1}. All mass balance closures of the results that follow were within 96% to 102%.

$$r_{gluc} = \frac{180}{232} r_{FA} + \frac{180}{92} r_{eth} + \frac{180}{6000} r_{O_2} + \frac{180}{184} r_{glyc} + \frac{180}{236} r_{SA} \quad (11)$$

Nitrogen feed rate investigation

In this study, three different nitrogen (urea) feed rates were investigated, namely 0, 0.625 and 1.875 mg.L^{-1}.h^{-1}. The experiments were performed in duplicate. Each repeat experiment was fitted with the model shown in the previous section. The model parameters for the repeat fermentations (r_{INIT}, A, Y_{FG}, Y_{FSA}) were then averaged and are shown in **Table 1**. The model parameters for each experiment are supplied with the supplementary material (Appendix A). The reactor was operated at a target dilution rate of 0.1 h^{-1}, although the actual outlet dilution rate varied slightly (< 5%) due to changes in the dosing and nitrogen feed rates. These small differences in dilution rate account for some of the dissimilarities seen in the repeat fermentations in **Figure 2** and **Figure 3**. However, these

small variations in dilution rate were taken into account since the inlet and outlet dilution rate were measured and their effects on the dissimilarities are removed in the results in **Table 1** and **Figure 4**. The measured dilution rates are shown in Appendix A. Small differences in biomass between repeat experiments also account for some of the differences in **Figure 2**, **Figure 3** and **Table 1**. Again, the biomass was measured (Appendix A) and the effect on the variance is removed in the mass-based rates in 4. The high dilution rate (0.1 h^{-1}) resulted in low FA titres and ensured that the nitrogen feed rate was the only significant variable affecting the metabolism of *R. oryzae*.

The FA and ethanol concentration profiles are shown in **Figure 2**. The decay of volumetric production rate is significant in the case where no nitrogen is being fed. Ethanol is considered to be an unwanted by-product [2,3] and numerous research studies aim at limiting ethanol production [3,12,16,25–28]. A decline in ethanol production is therefore beneficial if that in FA production is less severe. From **Figure 2** and **Table 1**, it is evident that the 0.625 $mg.L^{-1}.h^{-1}$ urea feed rate scenario is characterised by a slowly declining FA production rate and a fast declining ethanol production rate. The declines in the production rates are best interpreted by considering the fitted decay ratios (Table 1). It is very clear that urea addition has a significant effect on the decay of FA production as a seven-fold decrease in the decay factor (A_{FA}) was observed when urea was introduced into the system. In contrast, the effect on ethanol production is less severe as the decay factor (A_{ET}) decreased by only 40% when urea was introduced. For zero urea addition, A_{eth} was 3 times higher than the corresponding A_{FA}, but this value increased to 14 when urea was introduced (at 0.625 $mg.L^{-1}.h^{-1}$). Accordingly, it appears that an ideal production window exists at the end of the 0.625 $mg.L^{-1}.h^{-1}$ fermentation, where high FA and low ethanol production occurred.

Increasing the urea feed rate to 1.875 $mg.L^{-1}.h^{-1}$ resulted in an increase in the FA production rate (negative A_{FA}). The corresponding ethanol rate still decreased, but less severely than for the 0.625 $mg.L^{-1}.h^{-1}$ case. The increase in FA production is most probably linked to the increased biomass production which occurred, with the final biomass amount being 25% higher than in the zero urea case (Table 1). Ethanol production still exhibited a decline, although the decay factor (A_{ET}) was 4

times lower than in the 0.625 $mg.L^{-1}.h^{-1}$ urea fermentation. Ethanol production still remained significant towards the end of the fermentation.

During the production phase a significant fraction of the carbon uptake is used for respiration. The measured oxygen uptake given in **Figure 3** can be used to quantify the extent of respiration. Similar to the FA profile, an increase in urea feed rate to 0.625 $mg.L^{-1}.h^{-1}$ resulted in a significant decrease (60%) in the decay factor for oxygen (A_{O2}). This can be seen in **Figure 3** where the decay in oxygen consumption rate was less severe for the 0.625 $mg.L^{-1}.h^{-1}$ fermentation (middle graph on the left). Respiration, along with ethanol production, is responsible for generating the maintenance energy required for *R. oryzae* and the CO_2 produced during respiration can enhance the intracellular availability of CO_2 used to produce FA in the cytosol. Increasing the nitrogen feed rate to 1.875 $mg.L^{-1}.h^{-1}$ resulted in an increase in respiration as observed in the negative decay ratio (A_{O2}) in **Table 1**. This can be attributed to the observed biomass growth since a fraction of the respiration energy is invested in growth.

It was found that the glycerol and SA production rates were always proportional to the FA production rates (Supplementary material, Appendix B). This result is expected for SA given the single reaction step that separates SA from FA. The glycerol result is, however, less obvious given the branch point in glycolysis through which all the carbon fluxes. Generally, the amount of glycerol and SA produced is very small, being 3% to 5% the amount of FA.

The glucose profiles in **Figure 3** indicate that glucose consumption decreased with time, except for the 1.875 $mg.L^{-1}.h^{-1}$urea run. The theoretical lines on the glucose profiles were calculated via a mass balance, using the fitted profiles of the other metabolites. The agreement between the measurements and the calculated fit indicate good mass balance closures. This provides confidence in the accuracy of the measurements and suggests that all major metabolites are accounted for. Biomass growth was not incorporated into the mass balance. The agreement for the 1.875 $mg.L^{-1}.h^{-1}$urea run(< 2%) indicates that the fraction of glucose spent on biomass growth was minimal.

The main flux distribution as a function of time can be visualised by considering the distribution of the glucose flux. This was done by using the fitted rates (Equations 4, 5 and 6) and the stoichiometries in Equations 1, 2 and 3 to determine the amount of glucose consumed towards FA production (r_g^{FA}), ethanol production (r_g^{eth}) and respiration (r_g^{resp}). These three rates are then stacked on top of each other as seen in Figure 4. The relative size of each section gives an indication of the relative yield for the three main pathways. The right-hand graphs in Figure 4 give the instantaneous and accumulative yields. Note that the average of the two repeat runs is given with error bars indicating the variation.

It is evident that nitrogen addition inhibits the initial glucose consumption rate, with both urea fermentations starting at a value 60% lower than the zero urea fermentation. This stands in contrast to the decay of the total glucose consumption rate, where zero urea addition results in rapid decay. For ideal production conditions the thickness of the red stack (FA) should be maximised, while the thickness of the green stack (ethanol) should be minimised. For maximum urea addition (1.875 $mg.L^{-1}.h^{-1}$) the thickness of the red stack increases with time, but the green stack simply remains fairly thick. This results in a lower instantaneous yield of FA on glucose towards the end of the run when compared with the fermentation with lower urea addition (80% as against 90%). When the zero urea fermentation is compared with the lower urea fermentation, it is seen that the instantaneous yields and glucose productivity after 150 hours of operation are similar. The similarity will, however, not last for longer periods of operation given the faster rate of decay of the zero urea fermentation, in which FA production rates will diminish as time progresses. It is therefore advisable to prolong the duration of the lower urea run, as explained in the following section.

Even though it has been reported that nitrogen has a significant influence on the metabolism of *R. oryzae* during FA production [3], there have been limited studies [21,22] on this topic. Studies by Ding et al. [21] and Gu et al. [22], were performed with batch fermentations. The range of initial nitrogen (in the form of urea) concentration investigated for both these studies was between 0.1 $g.L^{-1}$ and 2 $g.L^{-1}$. The optimum initial nitrogen concentration for both these studies was 0.1 $g.L^{-1}$. Dividing the concentration by the fermentation length (70 hours) results in an average nitrogen feed rate of 1.43 $mg.L^{-1}.h^{-1}$. Since the optimum was found at the lower end of the range of concentrations

investigated, we can assume that the nitrogen feed rate that results in the highest yields and FA production rates could be lower than 1.43 $mg.L^{-1}.h^{-1}$. Unfortunately, the fermentation profiles were not shown in either report, which makes comparison of the FA and ethanol decay rates impossible. Although these studies found the same optimum nitrogen feed concentration, the reasoning behind the improved FA production was different. Ding et al.[21] showed that cytosolic fumarase was inhibited by the nitrogen in the feed medium, explaining why lower nitrogen concentrations in the feed result in increased FA production. Gu et al. [22] showed that nitrogen starvation stimulated the alternative respiration in *R. oryzae*, suggesting that the nitrogen concentration in the feed also affects the respiration efficiency. Enzyme assays for pyruvate carboxylase, considered to be rate limiting step in FA production [3,29,30], from *R. oryzae* show that it is inhibited by aspartate and glutamate, metabolites which require a nitrogen source for synthesis [30].

The studies described above clearly show that nitrogen plays a significant role in the control of the metabolism of *R. oryzae* and especially in the control of pyruvate carboxylase, fumarase and alternative oxidase. The issue with the nitrogen studies by Ding et al. [21] and Gu et al. [22] is that they were performed in batch fermentations in which the nitrogen concentration in the medium is expected to decrease over time and since the nitrogen levels directly influence the metabolism of *R. oryzae*. This effect is seen best in the study by Ding et al. [21] where the fumarase activity varied greatly during the fermentation. This study tried to address this issue with improved nitrogen control in order to prevent any nitrogen buildup. For example, as discussed above the average feed rate used [21] was 1.43 $mg.L^{-1}.h^{-1}$ which lies close to the 1.875 $mg.L^{-1}.h^{-1}$ feed rate used in this study. Therefore, by using similar nitrogen feed rates while changing the nitrogen feed method we managed to increase the accumulative yield from the 0.51 $g.g^{-1}$ obtained in [21] to 0.65 $g.g^{-1}$ after 75 hours. The results above clearly show that nitrogen control is crucial in creating a competitive FA process, and that simply limiting the nitrogen at the start of a batch fermentation is not sufficient. The results could also benefit the production of FA with *Sacchormyces cerevisiae* using heterologous genes from *R. oryzae*. Xu et al. [8] showed that nitrogen levels directly influenced the pyruvate carboxylase introduced into *S. cerevisiae* from *R. oryzae*, however, tests were performed in batch conditions and

therefore the nitrogen level was not properly controlled. Futher investigation on nitrogen control in *S. cerevisiae* could lead to improved yield and productivity as in the case of *R. oryzae*.

The yields obtained in the lower urea run (0.625 $mg.L^{-1}.h^{-1}$) become significant when compared with the thermodynamic analysis done on FA production by Taymaz-Nikerel et al. [31]. In this study attention was paid to the transport costs associated with FA production. It was found that an antiporter was the most likely transporter which results in a cost of 3 ATP per mol of FA transported from the cell. Using this assumption, together with zero ethanol production and along with a ATP/NADH ratio of 1.25 and a ATP/FADH ratio of 0.75, Taymaz-Nikerel et al. [31] predicted a maximum theoretical yield of 0.97 $g.g^{-1}$. This yield is very close to the instantaneous yield obtained at the end of the lower urea (0.625 $mg.L^{-1}.h^{-1}$) fermentation (0.9 $g.g^{-1}$) in this study. The slight difference in yield is caused by ethanol production as shown below. The high FA transport costs also explain why there is a significant amount of respiration (Figure 3) at the start of the zero urea fermentation.

When all of these results are taken into account, it seems that *R. oryzae* actively prioritises FA production in the nitrogen scarce environments found in this study. In the case where no nitrogen is added, *R. oryzae* uses the less efficient ethanol pathway in conjunction with respiration in order to produce the energy to produce and transport as much FA as possible before the organism starts to decay due to nitrogen starvation. When nitrogen is continuously added at a rate of 0.625 $mg.L^{-1}.h^{-1}$ *R. oryzae* uses more efficient pathways to produce the energy required for FA transportation while also ensuring that the FA production rate is kept stable over time. Further increasing the nitrogen feed rate to 1.875 $mg.L^{-1}.h^{-1}$ means that there is enough nitrogen available to increase the FA production by increasing the amount of biomass at the cost of the FA yield.

Dilution rate and long-term stability

A preliminary investigation was performed to determine the influence of the excreted catabolite concentrations on the response of *R. oryzae.* This was performed in conjunction with a long-term run (400 h) employing 0.625 $mg.L^{-1}.h^{-1}$ of urea addition. The lower urea addition rate was chosen based on the faster ethanol decay of the previous experiments and a more consistant biomass level compared

with higher urea feed rates. The dilution rate was first set to 0.1 h^{-1}, and was subsequently reduced to 0.05 h^{-1} and then to 0.025 h^{-1}. The measured concentrations and oxygen rates are given in Figure 5, where a clear increase in FA concentration and decrease in glucose outlet concentration are observed as the dilution rate is lowered. The changes in dilution were not reflected in the ethanol measurements owing to the rapid decay in ethanol production as observed in the previous results. The oxygen uptake rate also exhibited no sign of being affected by the dilution rate changes, with only a steady decay over time being observed.

A model as described in the previous sections was fitted over the whole time span, using only a single set of parameters as quantified in Table 2. The model is also shown in Figure 5. Note that the discontinuities in the model represent the sudden changes in dilution rate. Also note the similarities between the model parameters in Table 1 and those from the 0.625 $mg.L^{-1}.h^{-1}$urea run in Table 2. The proper fit of the single model indicates that the higher FA, SA and glycerol concentrations (see Appendix B) obtained at lower dilution rates have a negligible influence on the production characteristics of *R. oryzae* quantified by the model. This observation might not hold for FA concentrations higher than 14 $g.L^{-1}$, but it can be concluded that the catabolite concentration ranges considered in this study have no significant influence on the flux characteristics of the organism during FA production.

In Figure 6 the glucose rate distribution and yield characteristics are plotted in a fashion similar to that in Figure 4. It can be seen that ethanol production is virtually eliminated after 250 hours, leaving only FA production and respiration. It is encouraging to see that the thickness of the red stack (equivalent to the FA production rate) is not significantly reduced after 400 hours of operation, hinting that longer production is possible. After 400 hours the volumetric FA productivity was still 0.28 $g.L^{-1}.h^{-1}$, with zero ethanol as complement. This is highly favourable for the FA yield on glucose as can be seen in the yield graph which shows that a final instantaneous yield of 0.96 $g.g^{-1}$ and an accumulative yield of 0.81 $g.g^{-1}$were obtained. Longer operation will further improve the accumulative yield since the zero ethanol production phase will be prolonged. These yield results, in conjunction with an average

productivity of 0.36 $g.L^{-1}.h^{-1}$,compare favourably with those from other authors [3,12] who obtained accumulative yields of 0.3 $g.g^{-1}$to 0.6 $g.g^{-1}$ and average productivities of 0.3 $g.L^{-1}.h^{-1}$ to 0.5 $g.L^{-1}.h^{-1}$ for batch fermentations.

Conclusions

The results from the continuous fermentations clearly indicate how nitrogen addition influences the time-dependent product distribution of *R. oryzae*. A scenario was presented in which ethanol production terminated while FA volumetric production was on a par with the results in other literature reports. It was shown how the low urea addition rate (0.625 $mg.L^{-1}.h^{-1}$) resulted in high decay of the ethanol production rate and low decay of the FA production rate. A production window was presented where the FA yield on glucose was close to 1 $g.g^{-1}$while the FA volumetric productivity was 0.3 $g.L^{-1}.h^{-1}$. The results suggest that fermentation strategies with appropriate continuous nitrogen level control can be highly beneficial to the development of this process compared to simply limiting the nitrogen at the onset.

Funding

This work was supported by the Sugar Milling Research Institute Step-Bio program, South Africa; and the CSIR Inter-bursary program, South Africa.

Conflicts in interest

The authors do not declare any conflicts in interest.

References

[1] Werpy T, Petersen G, Aden A, Bozell J, Holladay J, White J, et al. Top Value Added Chemicals From Biomass. Volume 1-Results of Screening for Potential Candidates From Sugars and Synthesis Gas. DTIC Document; 2004.

[2] Roa Engel CA, Straathof AJJ, Zijlmans TW, van Gulik WM, van der Wielen L a M. Fumaric acid production by fermentation. Appl Microbiol Biotechnol 2008;78:379–89. doi:10.1007/s00253-007-1341-x.

[3] Xu Q, Li S, Huang H, Wen J. Key technologies for the industrial production of fumaric acid by fermentation. Biotechnol Adv 2012;30:1685–96. doi:10.1016/j.biotechadv.2012.08.007.

[4] Grand View Research. Maleic Anhydride Market Analysis By Application (Unsaturated Polyster Resins, BDO, Additives, Copolymers) and Segment Forecasts To 2020. 2014.

[5] Jang Y-S, Kim B, Shin JH, Choi YJ, Choi S, Song CW, et al. Bio-based production of C2-C6 platform chemicals. Biotechnol Bioeng 2012;109:2437–59. doi:10.1002/bit.24599.

[6] Xu Q, Li S, Fu Y, Tai C, Huang H. Two-stage utilization of corn straw by Rhizopus oryzae for fumaric acid production. Bioresour Technol 2010;101:6262–4. doi:10.1016/j.biortech.2010.02.086.

[7] Carta FS, Soccol CR, Ramos LP, Fontana JD. Production of fumaric acid by fermentation of

enzymatic hydrolysates derived from cassava bagasse. Bioresour Technol 1999;68:23–8. doi:http://dx.doi.org/10.1016/S0960-8524(98)00074-1.

[8] Xu G, Chen X, Liu L, Jiang L. Fumaric acid production in Saccharomyces cerevisiae by simultaneous use of oxidative and reductive routes. Bioresour Technol 2013;148:91–6. doi:10.1016/j.biortech.2013.08.115.

[9] Chen X, Wu J, Song W, Zhang L, Wang H, Liu L. Fumaric Acid Production by Torulopsis glabrata: Engineering the Urea Cycle and the Purine Nucleotide Cycle. Biotechnol Bioeng 2014;112:156–67. doi:10.1002/bit.25334.

[10] Du J, Cao N, Gong CS, Tsao GT, Yuan N. Fumaric acid production in airlift loop reactor with porous sparger. Appl Biochem Biotechnol 1997;63–65:541–56. doi:10.1007/BF02920452.

[11] Cao N, Du J, Chen C, Gong CS, Tsao GT. Production of fumaric acid by immobilized rhizopus using rotary biofilm contactor. Appl Biochem Biotechnol 1997;63–65:387–94. doi:10.1007/BF02920440.

[12] Roa Engel CA, van Gulik WM, Marang L, van der Wielen L a M, Straathof AJJ. Development of a low pH fermentation strategy for fumaric acid production by Rhizopus oryzae. Enzyme Microb Technol 2011;48:39–47. doi:10.1016/j.enzmictec.2010.09.001.

[13] Zhou Y, Du J, Tsao GT. Comparison of fumaric acid production by Rhizopus oryzae using different neutralizing agents. Bioprocess Biosyst Eng 2002;25:179–81. doi:10.1007/s004490100224.

[14] Kenealy W, Zaady ELI, Preez JCDU, Stieglitz B, Goldberg I, du Preez JC. Biochemical aspects of fumaric acid accumulation by Rhizopus arrhizus. Appl Environ Microbiol 1986;52:128–33.

[15] Naude A, Nicol W. Fumaric acid fermentation with immobilised Rhizopus oryzae : Quantifying time-dependent variations in catabolic flux. Process Biochem 2017;56:8–20.

doi:10.1016/j.procbio.2017.02.027.

[16] Zhou Y, Du J, Tsao GT. Mycelial pellet formation by Rhizopus oryzae ATCC 20344. Appl Biochem Biotechnol 2000;84–86:779–89.

[17] Liao W, Liu Y, Frear C, Chen S. A new approach of pellet formation of a filamentous fungus - Rhizopus oryzae. Bioresour Technol 2007;98:3415–23. doi:10.1016/j.biortech.2006.10.028.

[18] Fu Y, Xu Q, Li S, Chen Y, Huang H. Strain improvement of Rhizopus oryzae for over-production of fumaric acid by reducing ethanol synthesis pathway. Korean J Chem … 2010;27:183–6. doi:10.1007/s11814-009-0323-3.

[19] Huang L, Wei P, Zang R, Xu Z, Cen P. High-throughput screening of high-yield colonies of Rhizopus oryzae for enhanced production of fumaric acid. Ann Microbiol 2010;60:287–92. doi:10.1007/s13213-010-0039-y.

[20] Vaija J, Linko P. Continuous Citric Acid Production By Immobilized Aspergillus Niger: Reactor Performance and Fermentation Kinetics 1986;38:237–53.

[21] Ding Y, Li S, Dou C, Yu Y, Huang H. Production of fumaric acid by Rhizopus oryzae: role of carbon-nitrogen ratio. Appl Biochem Biotechnol 2011;164:1461–7. doi:10.1007/s12010-011-9226-y.

[22] Gu S, Xu Q, Huang H, Li S. Alternative respiration and fumaric acid production of Rhizopus oryzae. Appl Microbiol Biotechnol 2014;98:5145–52. doi:10.1007/s00253-014-5615-9.

[23] Ochsenreither K, Fischer C, Neumann A, Syldatk C. Process characterization and influence of alternative carbon sources and carbon-to-nitrogen ratio on organic acid production by Aspergillus oryzae DSM1863. Appl Microbiol Biotechnol 2014;98:5449–60. doi:10.1007/s00253-014-5614-x.

[24] Villadsen J, Nielsen J, Lidén G. Bioreaction Engineering Principles. Boston, MA: Springer US; 2011. doi:10.1007/978-1-4419-9688-6.

[25] Meussen BJ, de Graaff LH, Sanders JPM, Weusthuis R a. Metabolic engineering of Rhizopus oryzae for the production of platform chemicals. Appl Microbiol Biotechnol 2012;94:875–86. doi:10.1007/s00253-012-4033-0.

[26] Yu S, Huang D, Wen J, Li S, Chen Y, Jia X. Metabolic profiling of a Rhizopus oryzae fumaric acid production mutant generated by femtosecond laser irradiation. Bioresour Technol 2012;114:610–5. doi:10.1016/j.biortech.2012.03.087.

[27] Song P, Li S, Ding Y, Xu Q, Huang H. Expression and characterization of fumarase (FUMR) from Rhizopus oryzae. Fungal Biol 2011;115:49–53. doi:10.1016/j.funbio.2010.10.003.

[28] Wang G, Huang D, Qi H, Wen J, Jia X, Chen Y. Rational medium optimization based on comparative metabolic profiling analysis to improve fumaric acid production. Bioresour Technol 2013;137:1–8. doi:10.1016/j.biortech.2013.03.041.

[29] Overman SA, Romano a H. Pyruvate carboxylase of Rhizopus nigricans and its role in fumaric acid production. Biochem Biophys Res Commun 1969;37:457–63. doi:10.1016/0006-291X(69)90937-1.

[30] Osmani S a, Scrutton MC. The sub-cellular localisation and regulatory properties of pyruvate carboxylase from Rhizopus arrhizus. Eur J Biochem 1985;147:119–28.

[31] Taymaz-Nikerel H, Jamalzadeh E, Borujeni AE, Verheijen PT, Gulik WM van, Heijnen JJ. A thermodynamic analysis of dicarboxylic acid production in microorganisms. Biothermodynamics 2013:549–79.

Table 1: Model parameters for the nitrogen investigation. The parameter values are the average of the duplicate experiments. The standard errors are also shown.

	Urea feed rate ($mg.L^{-1}.h^{-1}$)		
Parameter	0	0.625	1.875
$r_{INIT_{FA}}$ ($g.L^{-1}.h^{-1}$)	0.72 ± 0.05	0.45 ± 0.01	0.49 ± 0.04
$r_{INIT_{O_2}}$ ($mmol.L^{-1}.h^{-1}$)	3.44 ± 0.15	2.79 ± 0.04	2.94 ± 0.11
$r_{INIT_{eth}}$ ($g.L^{-1}.h^{-1}$)	0.3 ± 0.001	0.21 ± 0.02	0.20 ± 0.03
A_{FA}	0.75% ± 0.01	0.09% ± 0.03	-0.40% ± 0.01
A_{O_2}	0.50% ± 0.01	0.21% ± 0.04	-0.16% ± 0.01
A_{eth}	2.30% ± 0.10	1.40% ± 0.01	0.37% ± 0.07
Y_{FG}	4.00% ± 0.01	4.40% ± 0.40	4.50% ± 0.40
Y_{FSA}	4.50% ± 0.01	3.60% ± 0.40	3.60% ± 0.70
Biomass ($g.L^{-1}$)	1.51 ± 0.10	1.65 ± 0.05	1.92 ± 0.06

Table 2: Model parameters for dilution rate investigation

Parameter	Value
$r_{MAX_{FA}}$ ($g.L^{-1}.h^{-1}$)	0.46
$r_{MAX_{O_2}}$ ($mmol.L^{-1}.h^{-1}$)	0.00113
$r_{MAX_{eth}}$ ($g.L^{-1}.h^{-1}$)	0.23
A_{FA}	0.12%
A_{O_2}	0.16%
A_{eth}	1.4%
Y_{FG}	4.8%
Y_{FSA}	3.2%
Biomass ($g.L^{-1}$)	1.70

Figure 1: Photos of the reactor setup.

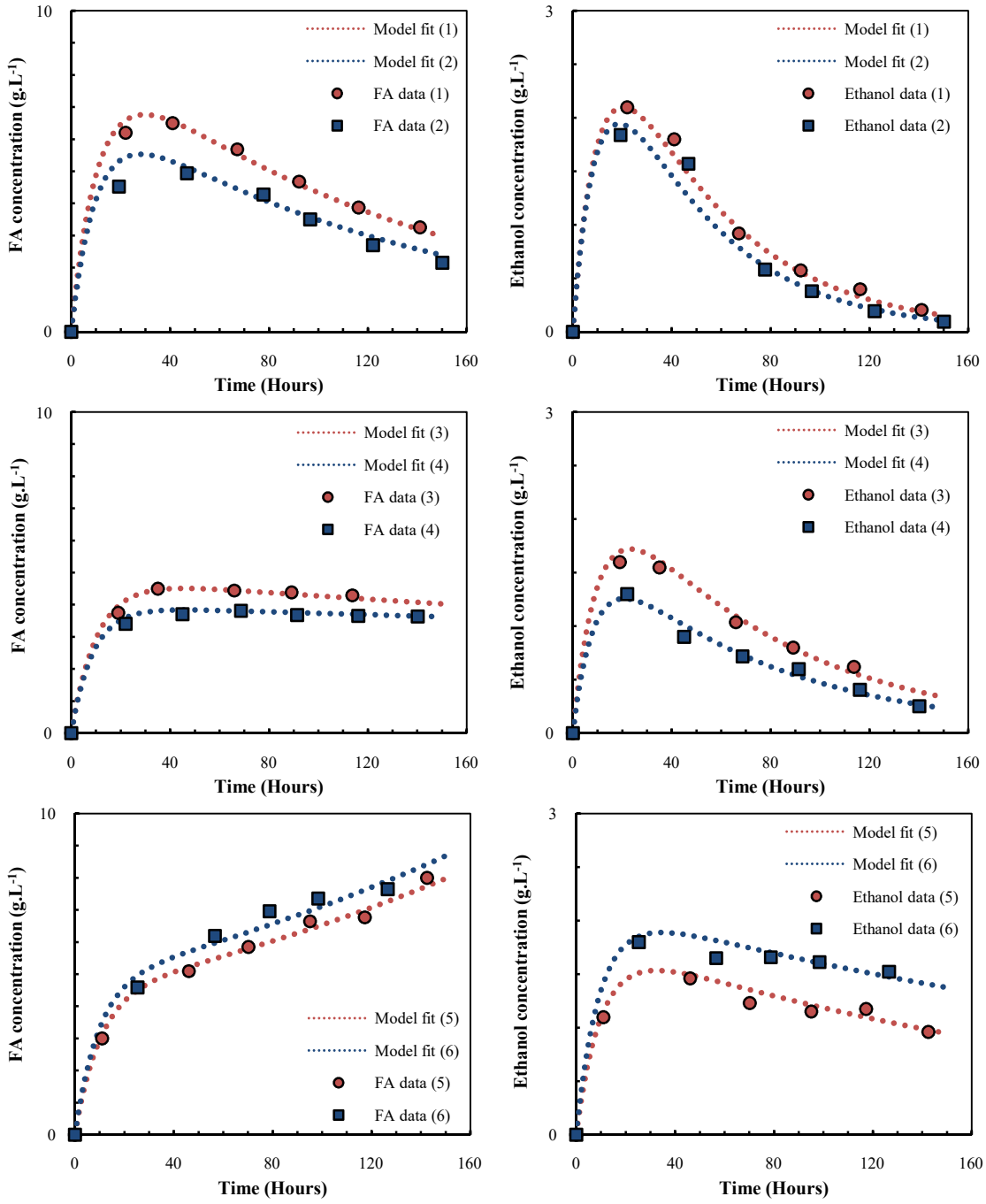

Figure 2: Fumaric acid (left) and ethanol (right) profiles for the nitrogen investigation with 0 $mg.L^{-1}h^{-1}$ (top), 0.625 $mg.L^{-1}h^{-1}$ (middle) and 1.875 $mg.L^{-1}h^{-1}$ (bottom) nitrogen addition. The dashed lines indicate the model fit.

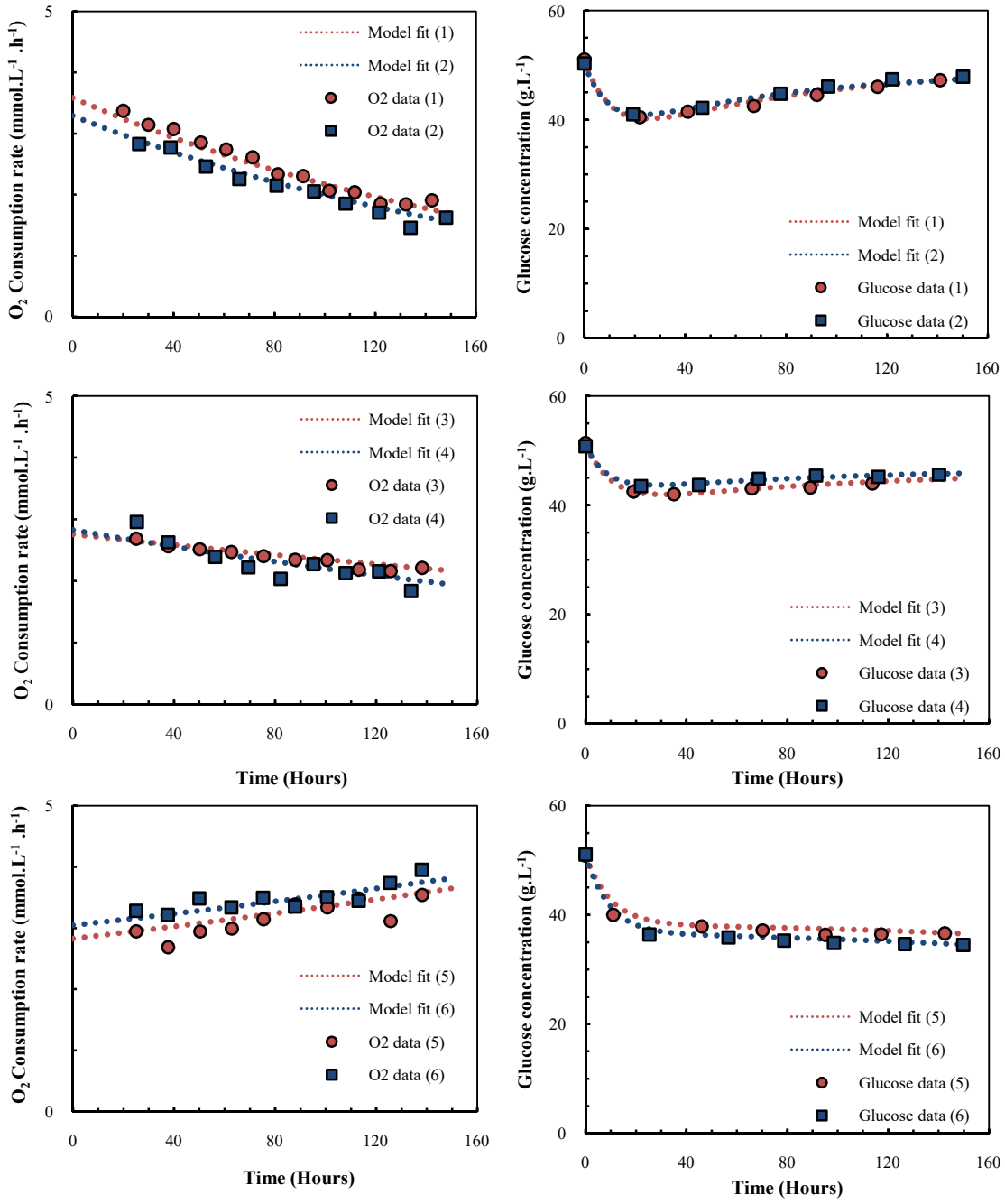

Figure 3:O_2 (left) and glucose (right) profiles for the nitrogen investigation with 0 $mg.L^{-1}h^{-1}$ (top), 0.625 $mg.L^{-1}h^{-1}$ (middle) and 1.875 $mg.L^{-1}h^{-1}$ (bottom) nitrogen addition. The dashed lines indicate the model fit.

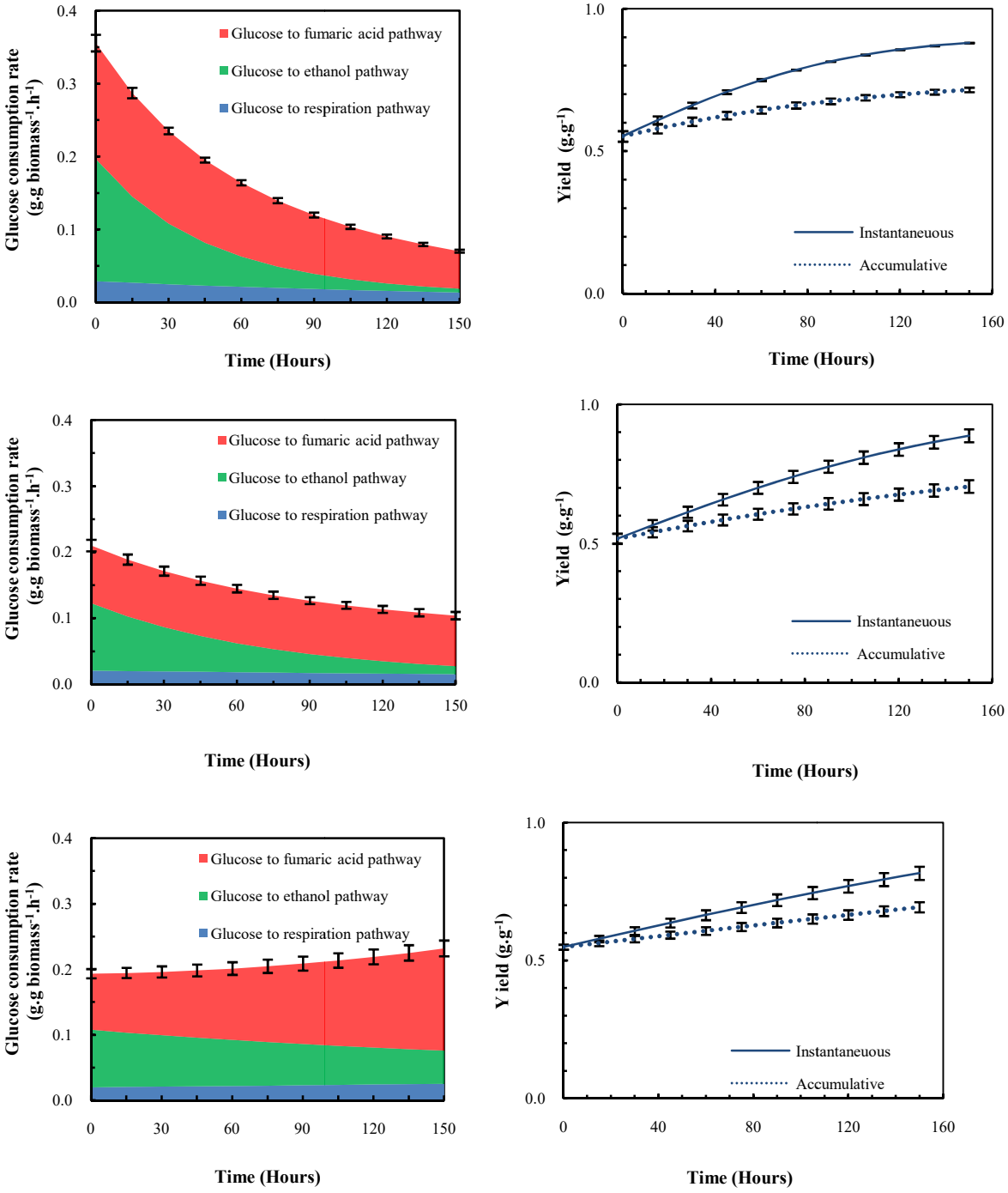

Figure 4: Glucose distribution profiles (left) and yield profiles (right) for the nitrogen investigation with 0 $mg.L^{-1}h^{-1}$ (top), 0.625 $mg.L^{-1}h^{-1}$ (middle) and 1.875 $mg.L^{-1}h^{-1}$ (bottom) nitrogen addition. The error bars show the standard errors for the repeat experiments.

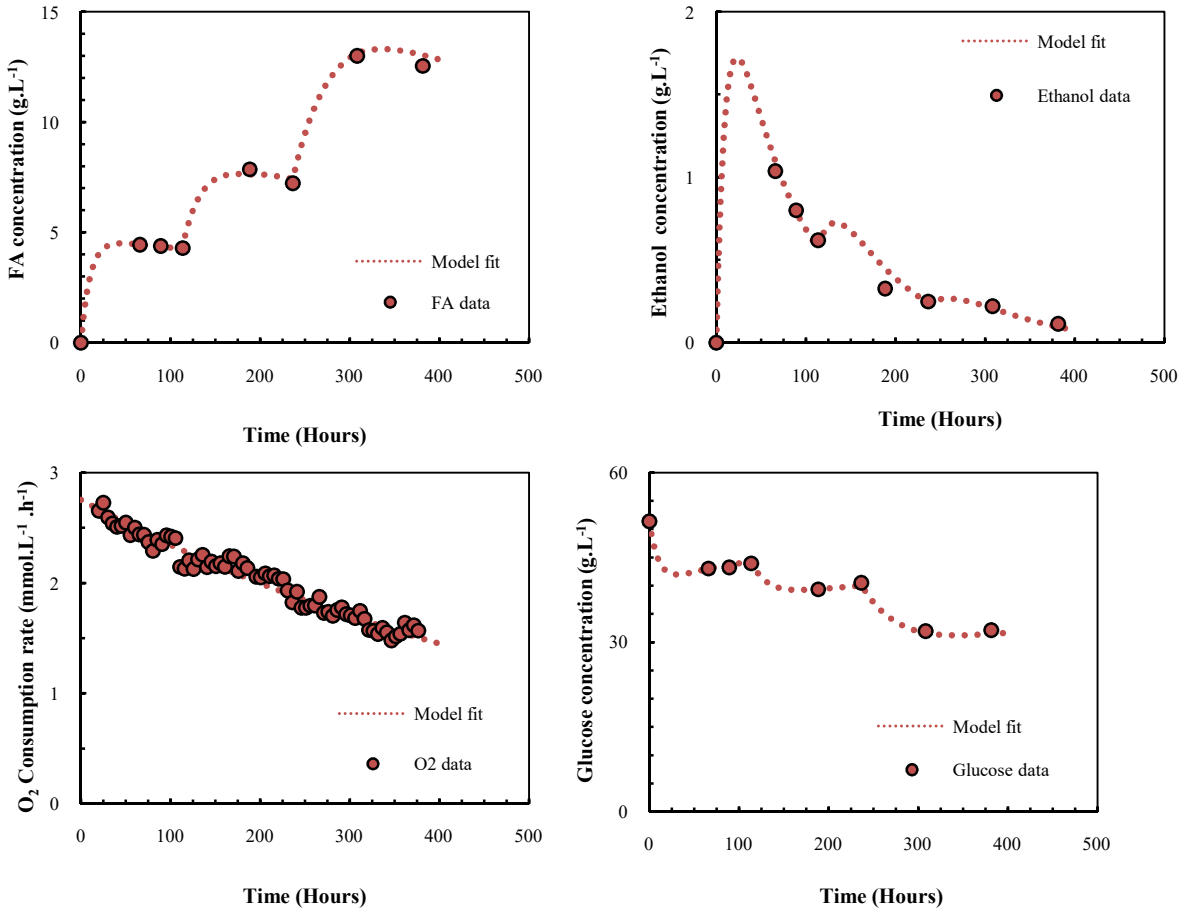

Figure 5: Fermentation profiles for the dilution rate investigation. Fumaric acid (top left), ethanol (top right), O_2 (bottom left) and glucose (bottom right).

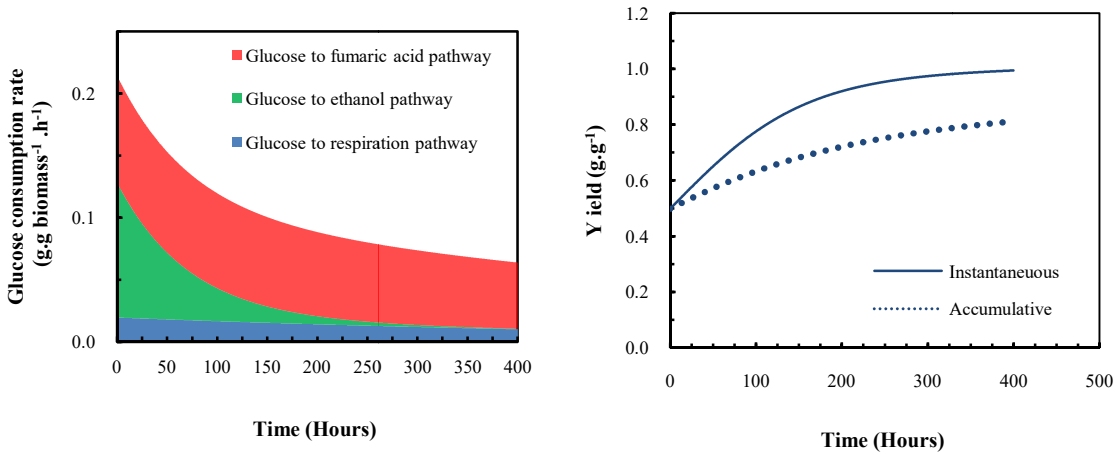

Figure 6: Glucose distribution profile (left) and yield profile (right) for the dilution rate investigation.

Appendix A: Fermentation data

The fermentation data for the nitrogen investigation experiments are shown in Table A.1 below.

Table A.1: Fermentation data of the nitrogen investigation experiments

0 mg.L^{-1}.h^{-1} urea feed rate		
	Fermentation	
	1	2
$r_{MAX_{FA}}$ (g.L^{-1}.h^{-1})	0.77	0.67
$r_{MAX_{O_2}}$ (mmol.L^{-1}.h^{-1})	3.59	3.29
$r_{MAX_{eth}}$ (g.L^{-1}.h^{-1})	0.30	0.30
A_{FA}	0.75%	0.75%
A_{O_2}	0.50%	0.50%
A_{eth}	2.20%	2.40%
Y_{FG}	4.00%	4.00%
Y_{FSA}	4.50%	4.50%
Biomass (g)	1.61	1.49
Average dilution rate (h^{-1})	0.091	0.098

0.625 mg.L^{-1}.h^{-1} urea feed rate		
	Fermentation	
	1	2
$r_{MAX_{FA}}$ (g.L^{-1}.h^{-1})	0.46	0.45
$r_{MAX_{O_2}}$ (mmol.L^{-1}.h^{-1})	2.76	2.83
$r_{MAX_{eth}}$ (g.L^{-1}.h^{-1})	0.23	0.19
A_{FA}	0.12%	0.06%
A_{O_2}	0.16%	0.25%
A_{eth}	1.40%	1.40%
Y_{FG}	4.80%	4.00%
Y_{FSA}	3.20%	4.00%
Biomass (g)	1.67	1.63
Average dilution rate (h^{-1})	0.093	0.110

1.875 mg.L^{-1}.h^{-1} urea feed rate		
	Fermentation	
	1	2
$r_{MAX_{FA}}$ (g.L^{-1}.h^{-1})	0.45	0.52
$r_{MAX_{O_2}}$ (mmol.L^{-1}.h^{-1})	2.83	3.05
$r_{MAX_{eth}}$ (g.L^{-1}.h^{-1})	0.18	0.22
A_{FA}	-0.40%	-0.40%
A_{O_2}	-0.17%	-0.15%
A_{eth}	0.45%	0.30%
Y_{FG}	3.80%	5.20%
Y_{FSA}	4.00%	3.20%
Biomass (g)	1.73	1.87
Average dilution rate (h^{-1})	0.090	0.096

Appendix B: Succinic acid and glycerol profiles

The profiles for SA and glycerol for the nitrogen investigation (Figure B-1) and dilution rate investigation (Figure B-2) are shown below.

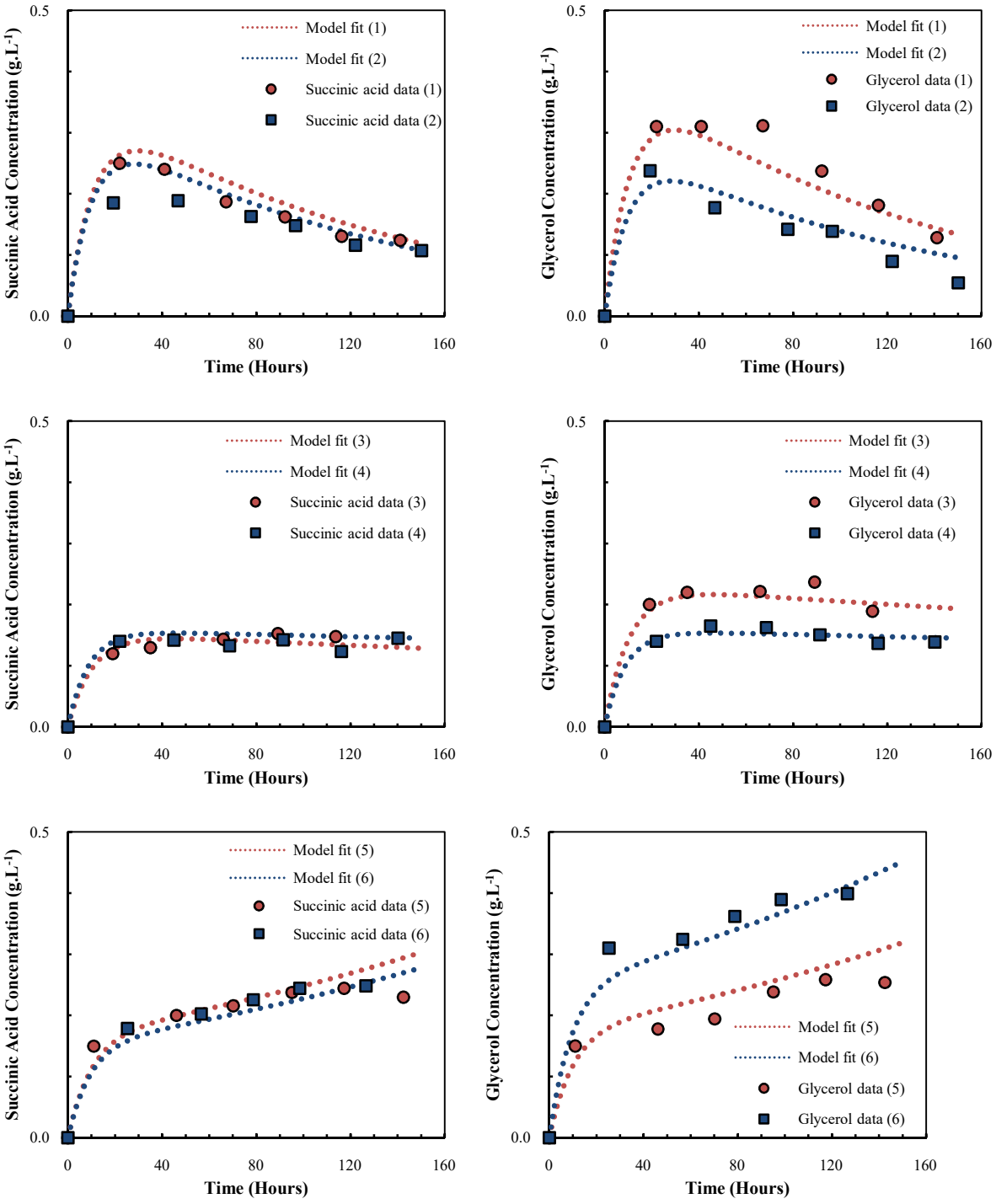

Figure B.1: Succinic acid (left) and glycerol (right) profiles for the nitrogen investigation with 0 $mg.L^{-1}h^{-1}$ (top), 0.625 $mg.L^{-1}h^{-1}$ (middle) and 1.875 $mg.L^{-1}h^{-1}$ (bottom) nitrogen addition. The dashed lines indicate the model fit.

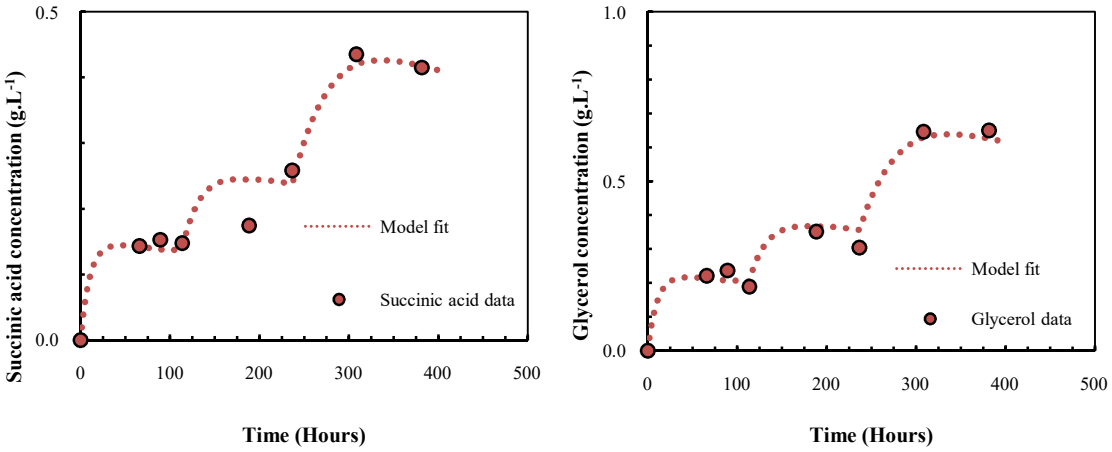

Figure B.2: Succinic acid (left) and glycerol (right) profiles for the dilution rate investigation. The dashed lines indicate the model fit.